Supporting Information

Self-Assembly of Giant Supramolecular Cubes with Terpyridine Ligands as Vertices and Metals on Edges

Chao Wang,[†,§] Xin-Qi Hao,[‡,§] Ming Wang,[†,*] Cunlan Guo,[#] Bingqian Xu,[#] Eric Tan,[†] Yan-Yan Zhang,[⊥] Yihua Yu,[⊥] Zhong-Yu Li,[⊻] Hai-Bo Yang,[⊻] Mao-Ping Song,[‡] Xiaopeng Li[†,*]

[†] Department of Chemistry and Biochemistry, Texas State University, San Marcos, TX 78666, United States

[‡] College of Chemistry and Molecular Engineering, Zhengzhou University, Zhengzhou 450052, P. R. China

[#] Single Molecule Study Laboratory, College of Engineering and Nanoscale Science and Engineering Center, University of Georgia, Athens, GA 30602, United States

[⊥] Shanghai Key Laboratory of Magnetic Resonance, Department of Physics, East China Normal University, Shanghai 200062, P. R. China

[⊻] Shanghai Key Laboratory of Green Chemistry and Chemical Processes, Department of Chemistry, East China Normal University, Shanghai 200062, P. R. China

Table of Contents

1. Experimental section

General procedures. Chemicals were purchased from Sigma/Aldrich, Fisher Scientific, or Alfa Aesar and used without further purification. Thin layer chromatography (TLC) was conducted on flexible sheets (Baker-flex) precoated with Al_2O_3 (IB-F) or SiO_2 (IB2-F) and the separated products were visualized by UV light. Column chromatography was conducted using basic Al_2O_3, Brockman Activity I (60-325 mesh) or SiO_2 (60-200 mesh) from Fisher Scientific. ^1H and ^{13}C NMR spectra were recorded on either a Bruker NMR 400 spectrometer or a Varian Mercury NMR 500 spectrometer, using $CDCl_3$ for ligand and CD_3CN for self-assemblies, except where noted. UV-vis spectra were recorded on a Perkin Elmer Lambda 35 UV-vis spectrometer. PL spectra were conducted on a Perkin Elmer LS55 luminescence spectrometer. For the AFM investigation, the sample was dissolved in CH_3CN at a concentration within the range 10^{-5} to 10^{-7} M. 1,3,5,-triphenyl-adamantane,[1] 1,3,5,-tri(4-iodophenyl)-adamantane,[2] 4'-(4-Boronatophenyl)-[2,2':6',2"]terpyridine[3] (**B1)** and 2-acetyl-4-*t*-butylpyridine[4] were synthesized according to literature procedure.

TWIM-MS measurements. The TWIM-MS experiments were performed using Waters Synapt G2 equipped with traveling wave ion mobility under the following conditions: ESI capillary voltage, 3kV; sample cone voltage, 30 V; extraction cone voltage, 3.5 V; source temperature 100 ^oC; desolvation temperature, 100 ^oC; cone gas flow, 10 L/h; desolvation gas flow, 700 L/h (N2); source gas control, 0 mL/min; trap gas control, 2 mL/min; Helium cell gas control, 100 mL/min; ion mobility (IM) cell gas control, 30 mL/min; sample flow rate, 5 μL/min; IM traveling wave height, 25 V; and IM traveling wave velocity, 1000 m/s. Q was set in rf-only mode to transmit all ions produced by ESI into the triwave region for the acquisition of TWIM MS data.

Collision cross section calibration. The calibration procedure of Scrivens et al[5] was used to convert the drift time scale of the TWIM MS experiments to a collision cross section (CCS) scale via the calibration curve was constructed by plotting the corrected CCSs of the molecular ions of ubiquitin (bovine red blood cells) and cytochrome C (horse heart), myoglobin[6] against the corrected drift times of the corresponding molecular ions measured in TWIM MS experiments at the same traveling wave velocity, traveling wave height, and ion mobility gas flow settings used for the, viz. 1000m/s, 25 V, and 30 mL/min, respectively.

Molecular modeling. Energy minimization of the supramolecular cubes was conducted with Materials Studio version 6.0, using the Anneal and Geometry Optimization tasks in the Forcite module (Accelrys Software, Inc.). All counterions are omitted. An initially energy-minimized structure was subjected to 70 annealing cycles with initial and mid-cycle temperatures of 50 and 1500 K, respectively, 20 heating ramps per cycle, 1000 dynamics steps per ramp, and one dynamics step per femtosecond. A constant volume/constant energy (NVE) ensemble was used and the geometry was optimized after each cycle. Geometry optimization used a universal force field with atom-based summation and cubic spline truncation for both the electrostatic and van der Waals parameters. 70 energy-minimized structures were selected for the calculation of theoretical collision cross sections using MOBCAL programs.

2. Synthesis and discussion of the related ligands and complexes

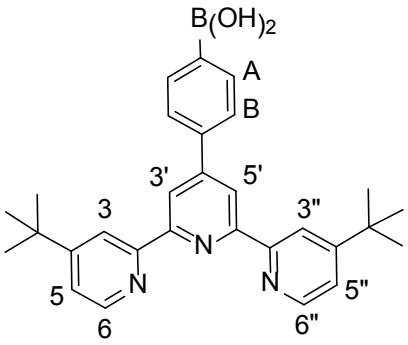

B2

B2: To a solution of 4-formylphenylboronic acid (1.31 g, 8.7 mmol) and 2-acetyl-4-*t*-butylpyridine (3.40 g, 19.2 mmol) in EtOH (30 mL), NaOH powder (2.10 g, 52.4 mmol) was added. After stirring at 25 °C for 10 h, aqueous ammonium hydroxide (20 mL, 30%) was added, and the mixture was kept refluxed for another 20 h. After cooling to room temperature, the volatiles were removed. 50 mL water was added to the residue, and the mixture was sonicated for 2 h. After centrifuge at 5000 rpm for 5 mins, the precipitate was collected and washed with $CHCl_3$ to give **B2** as bright yellow solid: 2.12 g (47%). ^{1}H NMR (400 MHz, Methanol-d_4) δ 8.84 (dd, J = 2.1, 0.8 Hz, 2H, tpy-$H^{3,3"}$), 8.77 (s, 2H, tpy-$H^{3',5'}$), 8.68 – 8.64 (m, 2H, tpy-$H^{6,6"}$), 7.92 (d, J = 8.3 Hz, 1H, Ph-H^{B}), 7.87 (d, J = 8.3 Hz, 1H, Ph-H^{A}), 7.55 (dd, J = 5.3, 2.0 Hz, 2H, tpy-$H^{5,5"}$), 1.51 (s, 18H). ^{13}C NMR (101 MHz, Methanol-d_4) δ 161.73, 155.80, 155.71, 150.32, 148.67, 139.09, 134.10, 125.87, 121.35, 121.25, 118.39, 118.23, 29.49, 16.95.

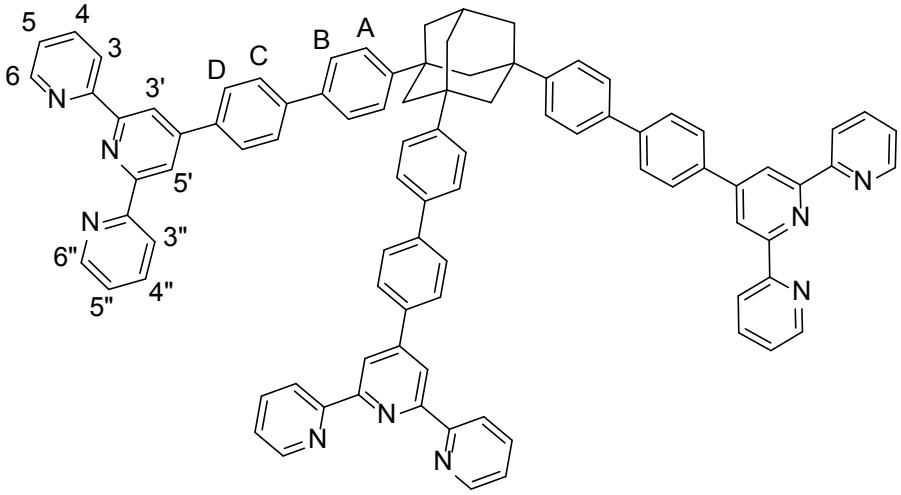

L1

L1: To a solution of 1,3,5,-tri(4-iodophenyl)-adamantane (422 mg, 569 µmol), $Pd_2(dba)_3$ (13 mg, 14 µmol), tri-tert-butylphosphine (12 mg, 59µmol) and 4'-(4-boronatophenyl)[2,2':6',2"]-terpyridine **B1** (707 mg, 1.99 mmol) in THF (45 mL) under nitrogen, aqueous K_2CO_3 (5 mL, 2 M) was added. After refluxing for 30 h, the mixture was cooled to room temperature and poured into an aq. $NaHCO_3$ solution (30 mL). The aqueous layer was extracted with $CHCl_3$, and the combined organic phase was washed with brine and dried over Na_2SO_4. After removal of solvent, the residue was purified by flash column chromatography (Al_2O_3), eluting with $CHCl_3$ to give **L1,** as a white solid: 173 mg (71%). ^{1}H NMR (400 MHz, Chloroform-*d*) δ 8.82 (s, 6H, tpy-$H^{3',5'}$), 8.76 (ddd, J = 4.8, 1.8, 0.9 Hz, 6H, tpy-$H^{3,3"}$), 8.70 (dt, J = 8.0, 1.1 Hz, 6H, tpy-$H^{6,6"}$), 8.06 – 7.98 (d, 6H, Ph-H^{D}), 7.90 (ddd, J = 8.0, 7.4, 1.8 Hz, 6H, tpy-$H^{5,5"}$), 7.82 – 7.75 (d, 6H, Ph-H^{C}), 7.75 – 7.67 (d, 6H, Ph-H^{B}), 7.67 – 7.58 (d, 6H, Ph-H^{A}), 7.37 (ddd, J = 7.5, 4.8, 1.2 Hz, 6H, tpy-$H^{4,4"}$), 2.66 (s, 1H), 2.27 (s, 6H), 2.14 (s, 6H). ^{13}C NMR (101 MHz, $CDCl_3$) δ 156.32, 149.83, 149.47, 149.15, 138.11, 137.13, 136.85, 127.72, 127.71, 127.49, 127.48, 127.04, 125.59, 123.81, 121.37, 118.71, 48.15, 41.53, 38.33, 30.24. HRMS (*m/z*): 429.5271 [**L1**+3H]$^{3+}$ (calcd 429.5278) and 644.7829 [**L1**+2H]$^{2+}$ (calcd 644.7838).

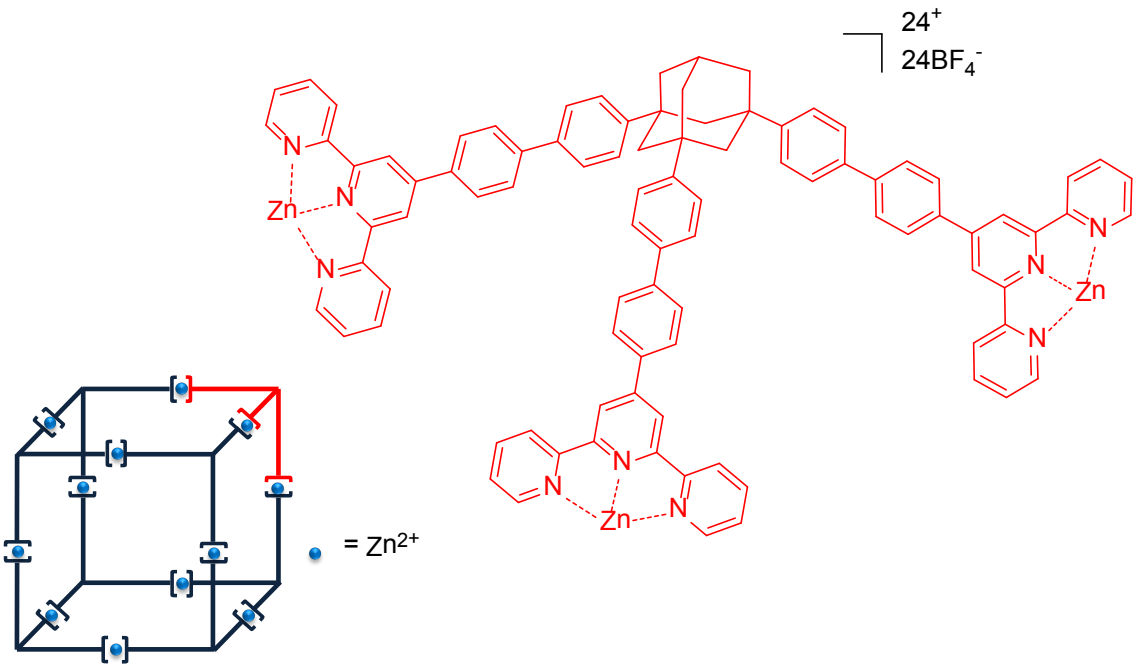

[$Zn_{12}L1_8$]

Cubic cage [$Zn_{12}L1_8$]: To a solution of ligand **L1** (9.1 mg, 7.1 μmol) in $CHCl_3$ (1 mL), a solution of $Zn(BF_4)_2$•$6H_2O$ (3.9 mg, 11.3 μmol) in MeOH (3 mL) was added; then the mixture was kept in a 60 °C sand bath for 7 h. After cooling to room temperature, the volatile was removed to give a white precipitate, which was sonicated, centrifuged and washed with water three times to give the crude white complex [$Zn_{12}L1_8$] with BF_4^- counterions. ESI MS (*m*/*z*): 1558.4 $[M\text{-}8BF_4^-]^{8+}$ (calcd *m*/*z*: 1558.0), 1375.6 $[M\text{-}9BF_4^-]^{9+}$ (calcd *m*/*z*: 1375.4), 1229.3 $[M\text{-}10BF_4^-]^{10+}$ (calcd *m*/*z*: 1228.2), 1109.7 $[M\text{-}11BF_4^-]^{11+}$ (calcd *m*/*z*: 1109.7), 1010.0 $[M\text{-}12BF_4^-]^{12+}$ (calcd *m*/*z*: 1010.0), 925.6 $[M\text{-}BF_4^-]^{13+}$ (calcd *m*/*z*: 925.7), 853.6 $[M\text{-}14BF_4^-]^{14+}$ (calcd *m*/*z*: 853.6), 790.6 $[M\text{-}15BF_4^-]^{15+}$ (calcd *m*/*z*: 790.9), 735.7 $[M\text{-}16BF_4^-]^{16+}$ (calcd *m*/*z*: 735.8), and 687.2 $[M\text{-}17BF_4^-]^{17+}$ (calcd *m*/*z*: 687.3).

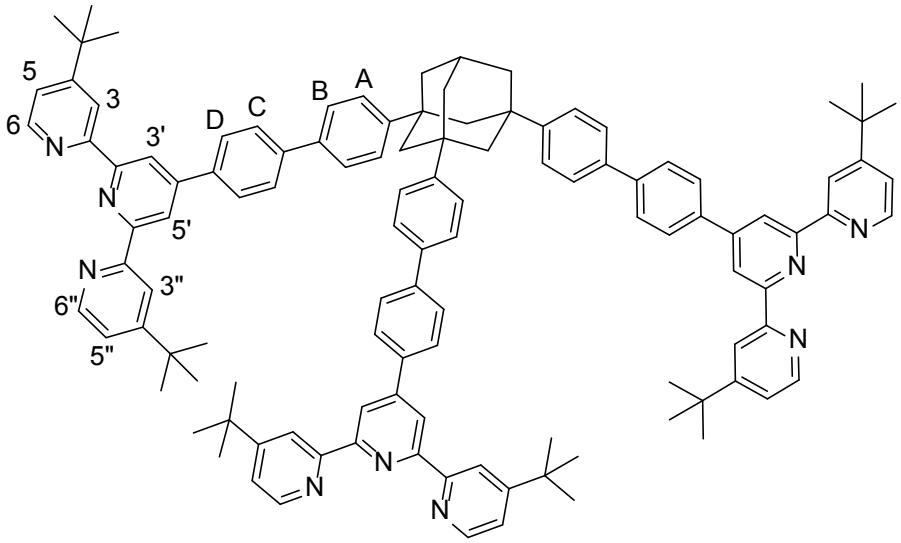

L2

L2: To a solution of 1,3,5,-tri(4-iodophenyl)-adamantane (389 mg, 524 μmol), $Pd_2(dba)_3$ (15 mg, 16 μmol), tri-tert-butylphosphine (14 mg, 69μmol) and **B2** (1.02 g, 2.19 mmol) in THF (45 mL) under nitrogen, aqueous K_2CO_3 (5 mL, 2 M) was added. After refluxing for 30 h, the mixture was cooled to room temperature and poured into an aq. $NaHCO_3$ solution (30 mL). The aqueous layer was extracted with $CHCl_3$, and the combined organic phase was washed with brine and dried over Na_2SO_4. After removal of solvent, the residue was purified by flash column chromatography (Al_2O_3), eluting with $CHCl_3$ to give **L2,** as a yellow solid: 184 mg (65%). ^{1}H NMR (400 MHz, Chloroform-*d*) δ 8.84 (dd, *J* = 2.0, 0.8 Hz, 6H, tpy-$H^{3,3"}$), 8.82 (s, 6H, tpy-$H^{3',5'}$), 8.68 (dd, *J* = 5.2, 0.7 Hz, 6H, tpy-$H^{6,6"}$), 8.04 (d, *J* = 8.5 Hz, 6H, Ph-H^{D}), 7.79 (d, *J* = 8.5 Hz, 6H, Ph-H^{C}), 7.72 (d, *J* = 8.5 Hz, 6H, Ph-H^{B}), 7.64 (d, *J* = 8.5 Hz, 6H, Ph-H^{A}), 7.39 (dd, *J* = 5.3, 2.0 Hz, 6H, tpy-$H^{5,5"}$), 2.67 (s, 1H), 2.29 (s, 6H), 2.16 (s, 6H), 1.48 (s, 54H). ^{13}C NMR (101 MHz, $CDCl_3$) δ 160.72, 156.17, 156.03, 149.84, 149.45, 149.09, 141.51, 138.14, 137.21, 127.74, 127.44, 127.04, 125.58, 121.06, 118.45, 118.26, 48.16, 41.54, 38.33, 34.99, 30.56, 25.75. HRMS (m/z): 541.6524 [**L2**+3H]$^{3+}$ (calcd 541.6530) and 811.9713 [**L2**+2H]$^{2+}$ (calcd 811.9716).

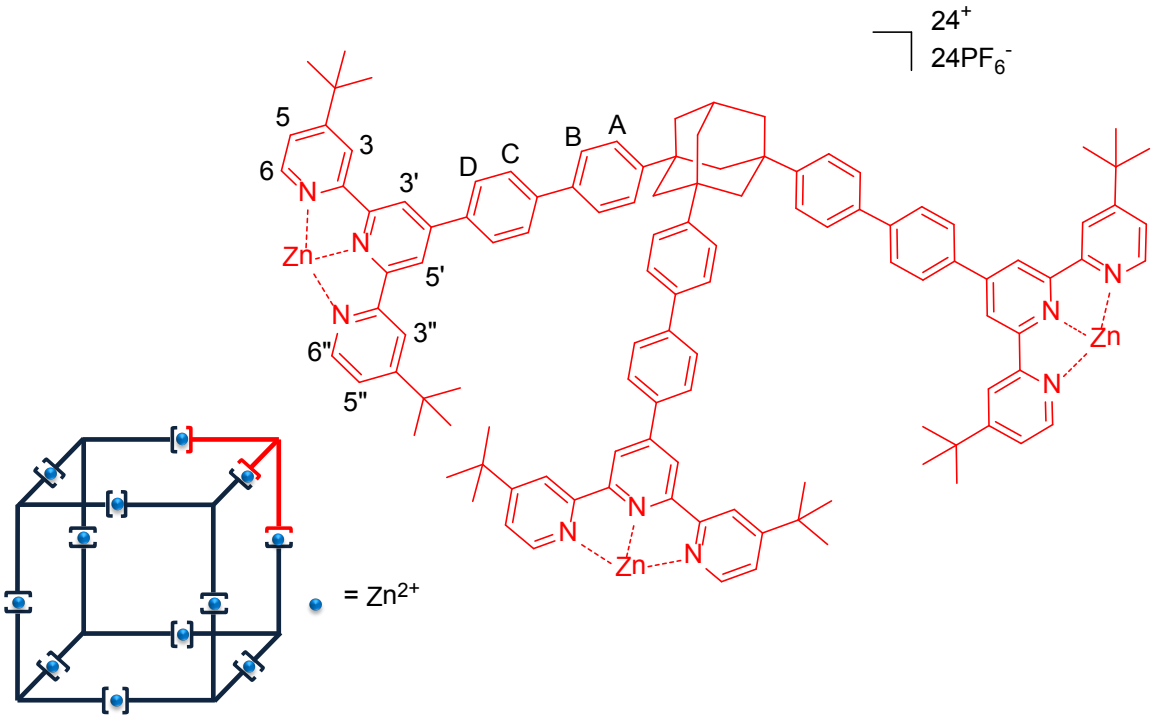

[$Zn_{12}L2_8$]

Cubic cage [**$Zn_{12}L2_8$**]: To a solution of ligand **L2** (10.0 mg, 6.2 μmol) in $CHCl_3$ (1 mL), a solution of $Zn(NO_3)_2$•$6H_2O$ (2.5 mg, 8.3 μmol) in MeOH (3 mL) was added; then the mixture was kept in a 60 °C sand bath for 7 h. After cooling to room temperature, excess NH_4PF_6 (around 200 mg) was added to generate a white precipitate, which was sonicated, centrifuged and washed with MeOH and then water three times to give the crude white complex [**$Zn_{12}L2_8$**] with PF_6^- counterions: 10.9 mg (82%). ^{1}H NMR (400 MHz, Acetonitrile-d_3) δ 9.12 (s, 16H, tpy-$H^{3',5'}$), 8.69 (s, 16H, tpy-$H^{3,3''}$), 8.35 (s, 16H, Ph-H^{D}), 8.08 (s, 16H, Ph-H^{C}), 7.90 (s, 16H, Ph-H^{B}), 7.75 (m, J = 14.4 Hz, 32H, tpy-$H^{6,6''}$ and Ph-H^{A}), 7.41 (s, 16H, tpy-$H^{5,5''}$), 1.37 (s, 144H). ^{13}C NMR (126 MHz, Acetonitrile-d_3) δ 166.15, 150.04, 147.96, 131.85, 128.95, 127.74, 127.07, 126.05, 125.07, 124.32, 121.27, 118.12, 38.42, 35.59, 29.42. ESI MS (*m*/*z*): 1292.0 [M-$12PF_6^-$]$^{12+}$ (calcd *m*/*z*:1292.0), 1181.4 [M-$13PF_6^-$]$^{13+}$ (calcd *m*/*z*: 1181.4), 1086.7 [M-$14PF_6^-$]$^{14+}$ (calcd *m*/*z*: 1086.7), 1004.5 [M-$15PF_6^-$]$^{15+}$ (calcd *m*/*z*: 1004.5), 932.7 [M-$16PF_6^-$]$^{16+}$

(calcd *m*/*z*: 932.6), 869.3 $[M\text{-}17PF_6^-]^{17+}$ (calcd *m*/*z*: 869.3), 812.9 $[M\text{-}18PF_6^-]^{18+}$ (calcd *m*/*z*: 812.9), and 762.4 $[M\text{-}19PF6^-]^{19+}$ (calcd *m*/*z*: 762.4).

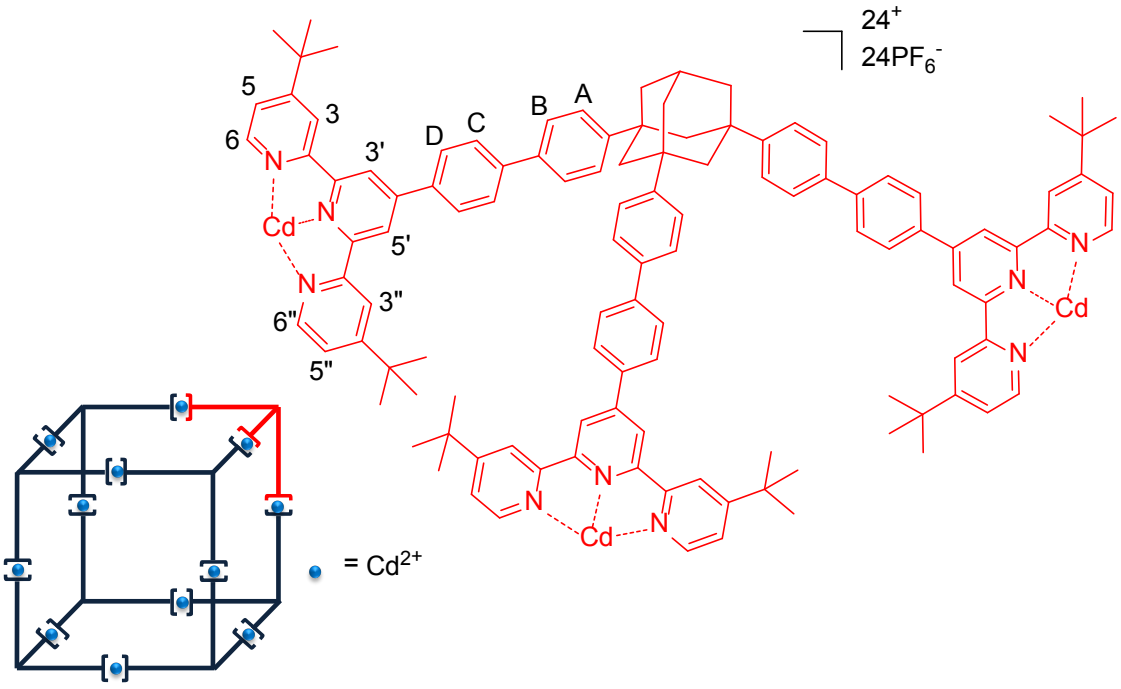

[$Cd_{12}L2_8$]

Cubic cage [$Cd_{12}L2_8$]: To a solution of ligand **L2** (10.2 mg, 6.3 μmol) in $CHCl_3$ (1 mL), a solution of $Cd(NO_3)_2$•$4H_2O$ (2.7 mg, 8.5 μmol) in MeOH (3 mL) was added; then the mixture was kept in a 60 °C sand bath for 3 h. After cooling to room temperature, excess NH_4PF_6 (around 200 mg) was added to generate a white precipitate, which was sonicated, centrifuged and washed with MeOH and then water three times to give the crude white complex [$Cd_{12}L2_8$] with PF_6^- counterions: 12.5 mg (90%). ^{1}H NMR (400 MHz, Acetonitrile-d_3) δ 9.03 (s, 16H, tpy-$H^{3',5'}$), 8.68 (s, 16H, tpy-$H^{3,3''}$), 8.31 (s, 16H, Ph-H^{D}), 8.05 (s, 16H, Ph-H^{C}), 7.95 (s, 16H, tpy-$H^{6,6''}$), 7.86 (s, 16H, Ph-H^{B}), 7.75 (s, 16H, Ph-H^{A}), 7.50 (s, 16H, tpy-$H^{5,5''}$), 1.39 (s, 144H). ^{13}C NMR (126 MHz, Acetonitrile-d_3) δ 166.19, 150.49, 149.25, 148.90, 137.11, 135.09, 128.92, 127.66, 127.05, 126.04, 124.19, 121.68, 121.04, 38.36, 35.61, 29.44. ESI MS (*m*/*z*): 1474.0 [M-

11PF_6^-]$^{11+}$ (calcd *m*/*z*:1474.0), 1339.1 [M-12PF_6^-]$^{12+}$ (calcd *m*/*z*: 1339.1), 1224.8 [M-13PF_6^-]$^{13+}$ (calcd *m*/*z*: 1224.8), 1127.0 [M-14PF_6^-]$^{14+}$ (calcd *m*/*z*: 1127.0), 1042.1 [M-15PF_6^-]$^{15+}$ (calcd *m*/*z*: 1042.1), 967.9 [M-16PF_6^-]$^{16+}$ (calcd *m*/*z*: 967.9), 902.4 [M-17PF_6^-]$^{17+}$ (calcd *m*/*z*: 902.4), 844.2 [M-18PF6$^-$]$^{18+}$ (calcd *m*/*z*: 844.2), 792.1 [M-19PF_6^-]$^{19+}$ (calcd *m*/*z*: 792.1), 745.2 [M-20PF_6^-]$^{20+}$ (calcd *m*/*z*: 745.3), and 702.8 [M-21PF_6^-]$^{21+}$ (calcd *m*/*z*: 702.8).

3. ESI MS, ESI TWIM MS plots

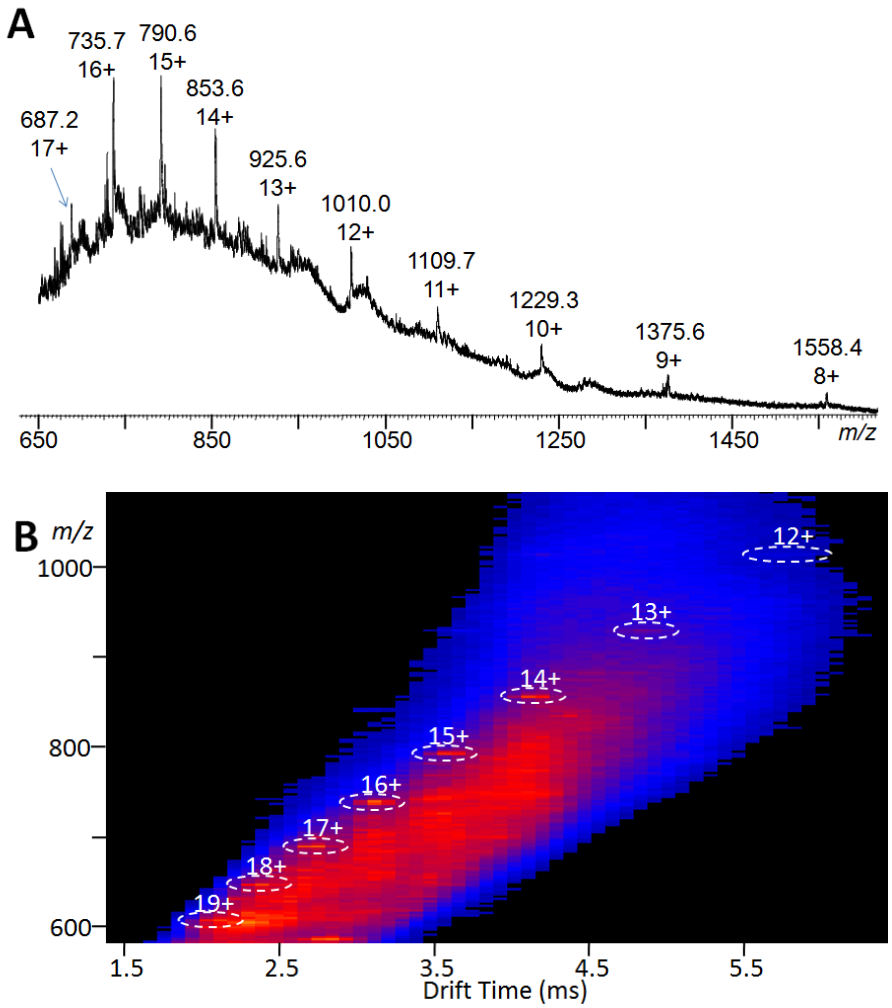

Figure S1. (A) ESI mass spectrum and (B) 2D ESI-TWIM-MS plot (*m/z* vs drift time) for [$\mathbf{Zn_{12}L1_8}$]. The charge states of intact assemblies are marked.

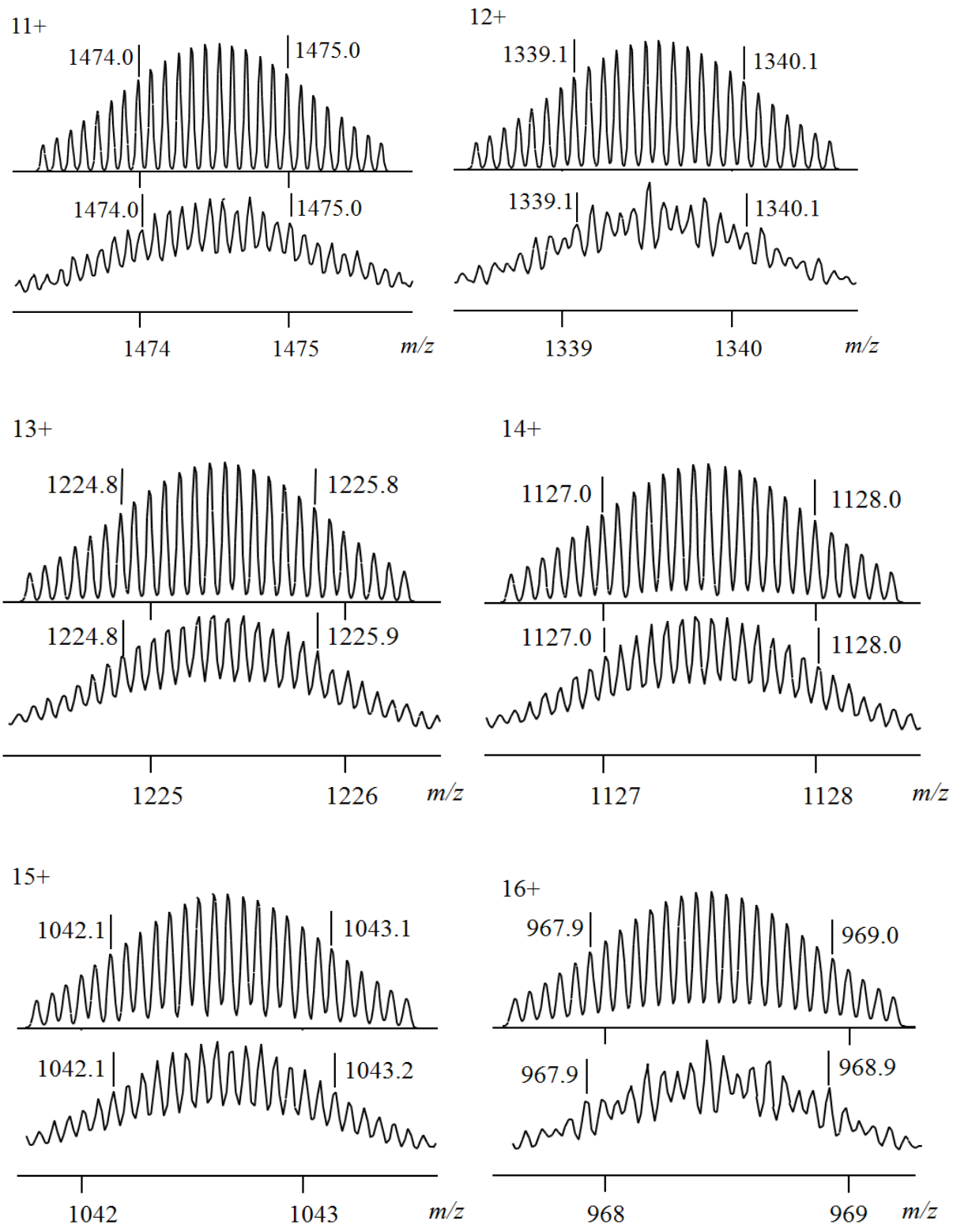

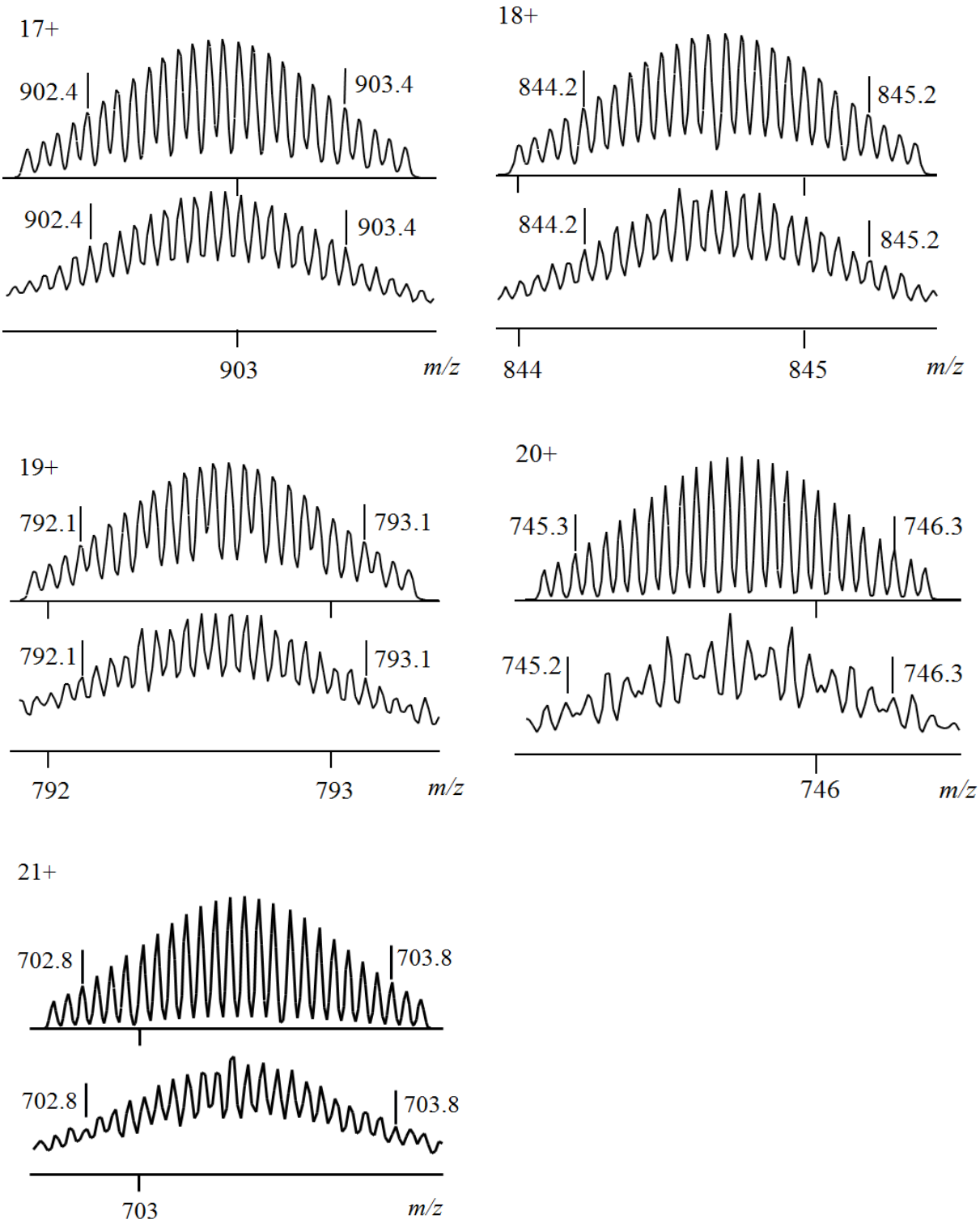

Figure S2. Calculated (top) and measured (bottom) isotope patterns for the different charge states (11+ to 21+) observed from [$\mathbf{Cd_{12}L2_8}$] (PF_6^- as counterion).

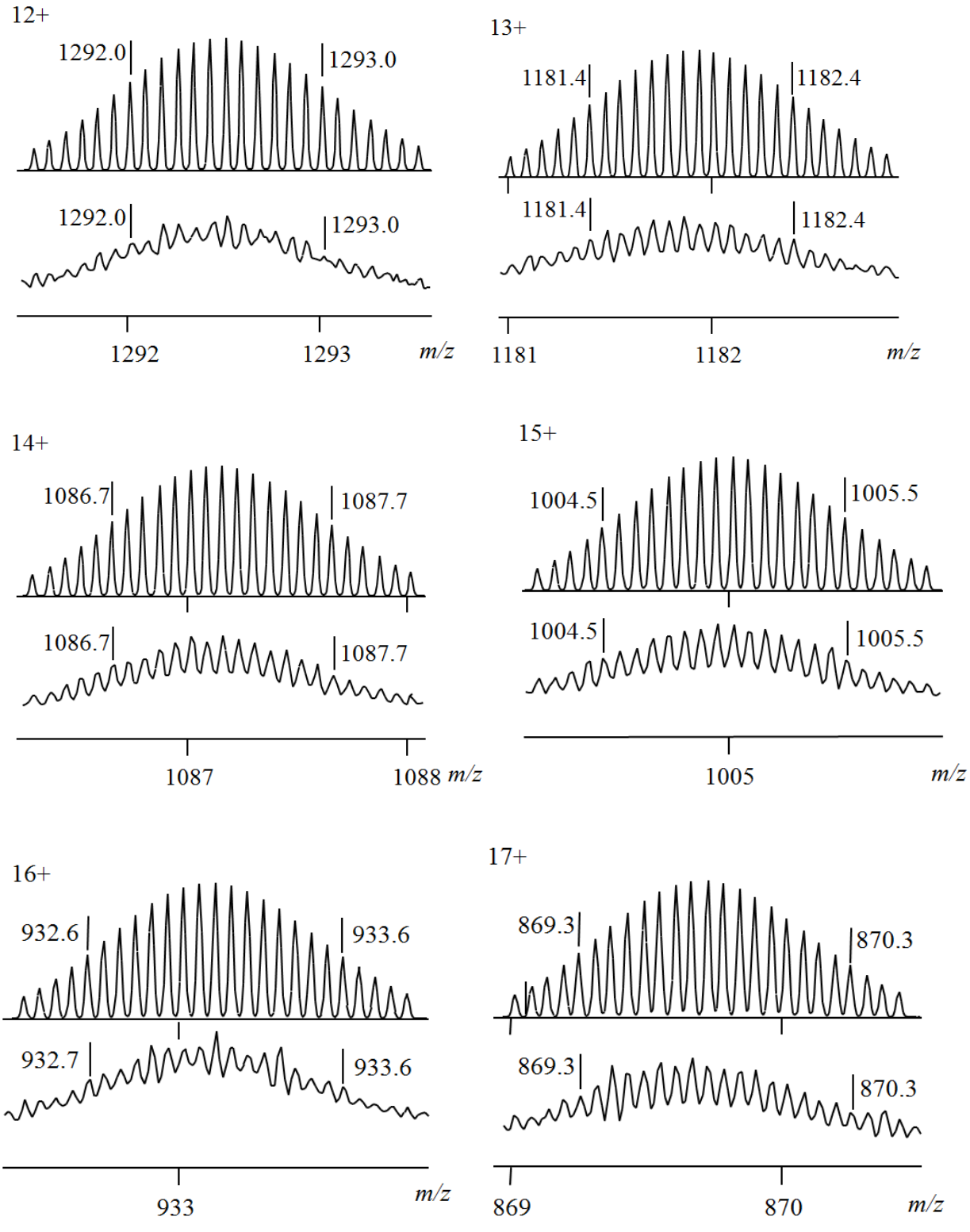

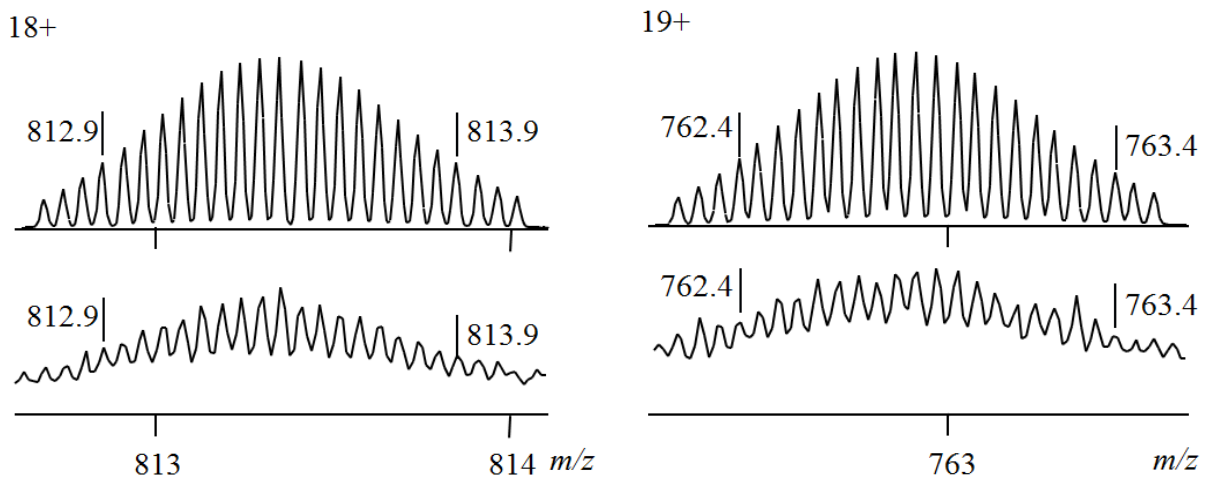

Figure S3. Calculated (top) and measured (bottom) isotope patterns for the different charge states (12+ to 19+) observed from [$\mathbf{Zn_{12}L2_8}$] (PF_6^- as counterion).

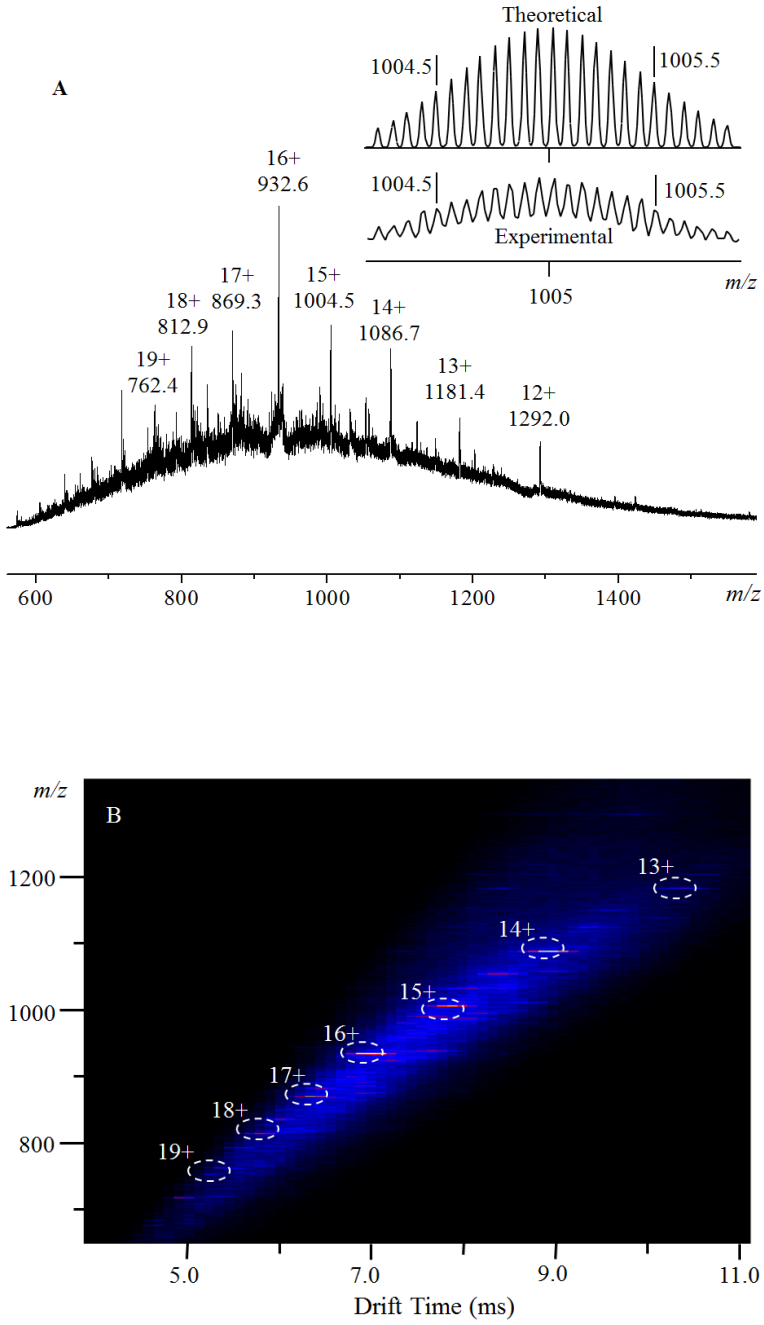

Figure S4. (A) ESI mass spectrum and (B) 2D ESI-TWIM-MS plot (*m/z* vs drift time) for [$\mathbf{Zn_{12}L2_8}$]. The charge states of intact assemblies are marked.

4. Calibration of drift time scale

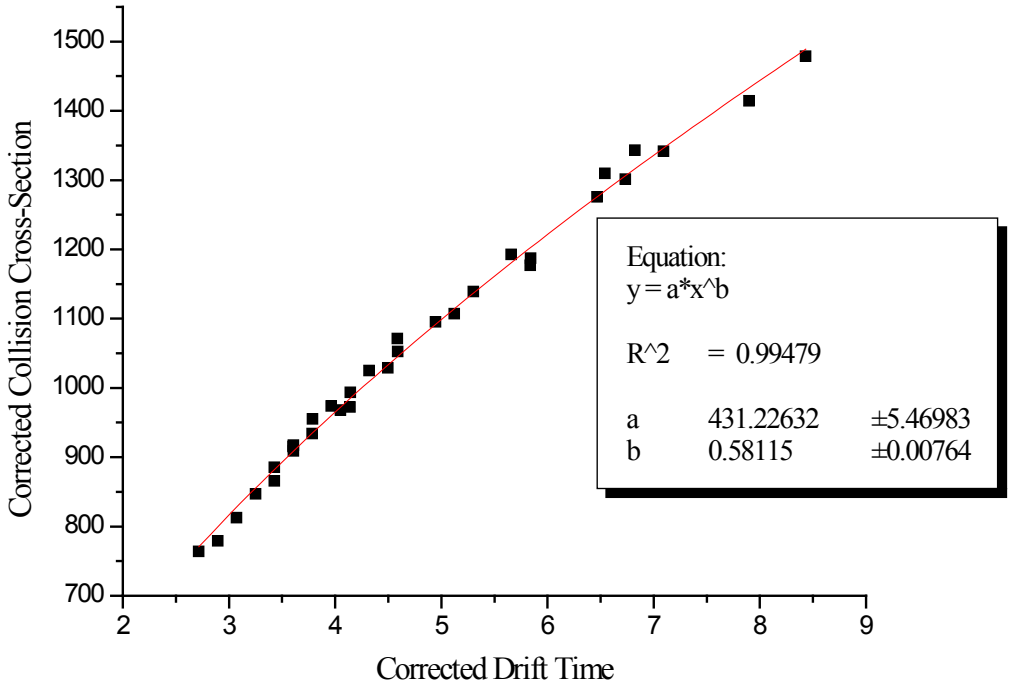

Figure S5. Plot of corrected drift times (arrival times) against corrected published cross sections for the multiply charged ions arising from ubiquitin (bovine red blood cells) and cytochrome C (horse heart), myoglobin. Drift times were measured at a traveling wave velocity of 1000 m/s and a traveling wave height of 25 V. This calibration plot was utilized to obtain the experimental collision cross sections (CCSs) listed in **Table 1**. Corrected drift times (x-axis values) and corrected collision cross-sections (y-axis values) are reproducible within <±1.3% and < ±1.3%, respectively.

5. Molecular modeling results

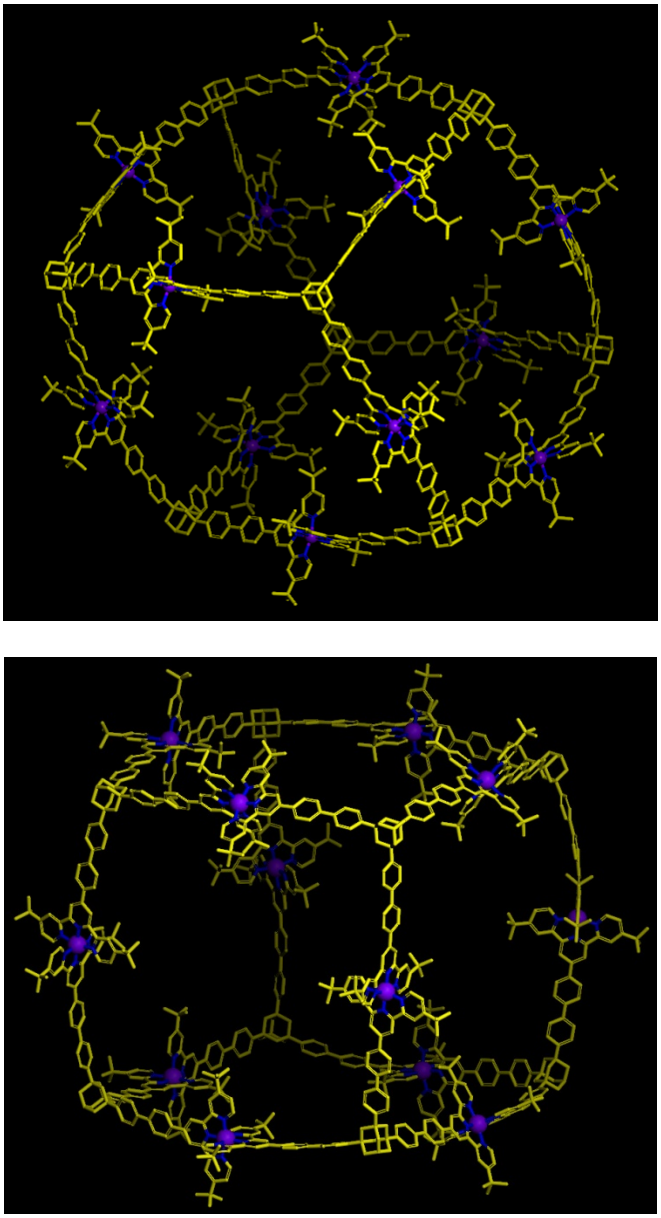

Figure S6. Representative energy-minimized structures of [$\mathbf{Cd_{12}L2_8}$].

6. Photo-physical properties of ligand and complexes

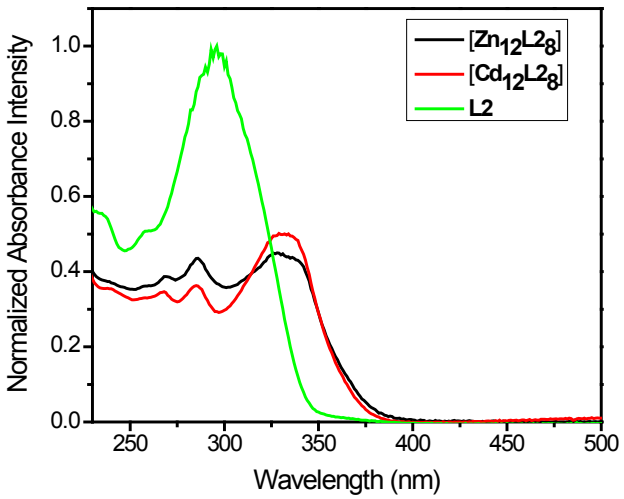

Figure S7. Absorption spectra of complexes in MeCN and ligand **L2** in $CHCl_3$ (10^{-6} M) at 25 °C.

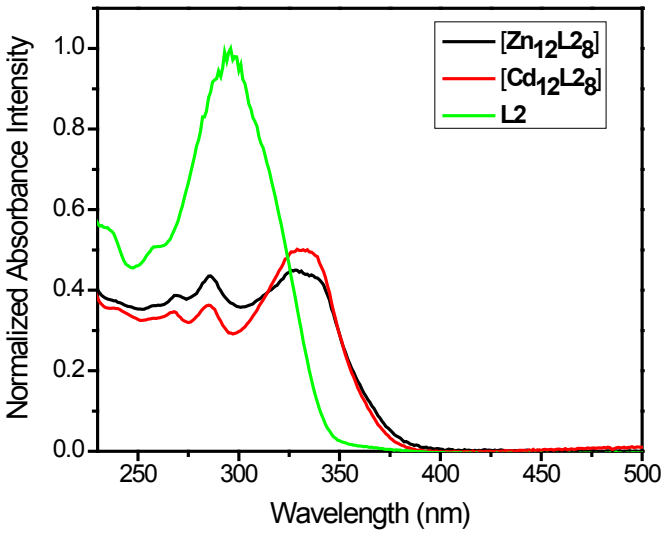

Figure S8. Absorption spectra of complexes and ligand **L2** in solid state at 25 °C.

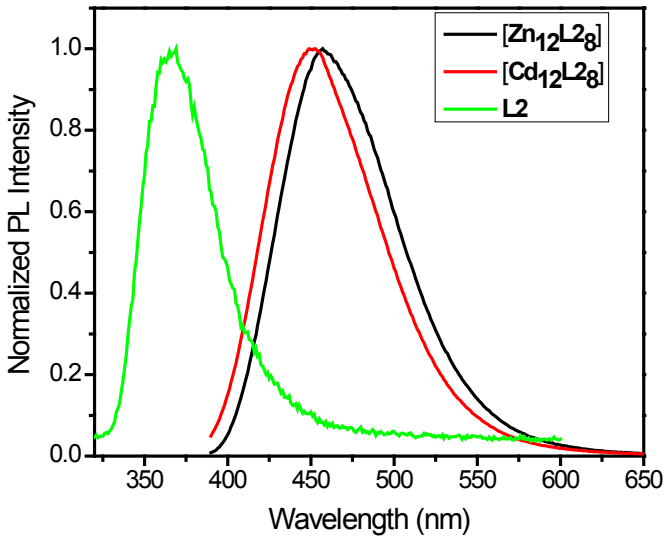

Figure S9. Emission spectra of complexes in MeCN and ligand **L2** in $CHCl_3$ (10^{-6} M) at 25 °C.

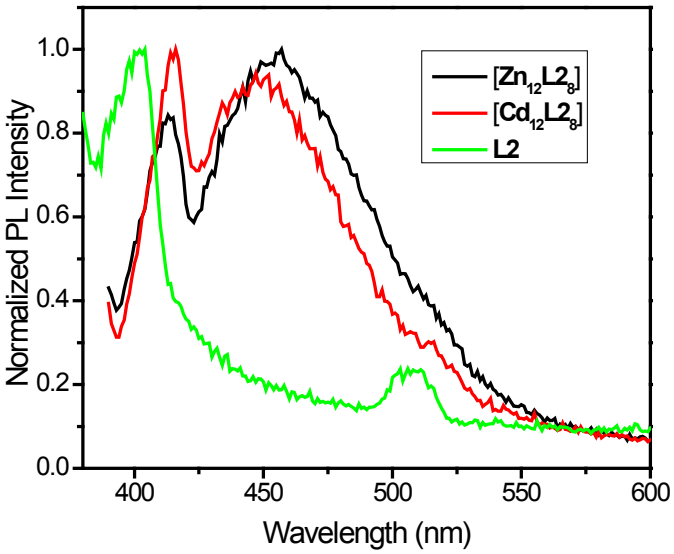

Figure S10. Emission spectra of complexes and ligand **L2** in solid state at 25 °C.

Table S1. Photophysical properties of complexes and corresponding ligand **L2** at 25 °C.

Compounds	λ_{max} absorption (sol., nm)	λ_{max} emission (sol., nm)	λ_{max} absorption (film, nm)	λ_{max} emission (film, nm)
[$\mathbf{Cd_{12}L2_8}$]	285, 332	452	285, 332	452, 415
[$\mathbf{Zn_{12}L2_8}$]	286, 328	457	286, 330	457, 413
L2	296	369	303	403

7. ^{1}H NMR, ^{13}C NMR, COSY and HSQC NMR spectra, AFM data

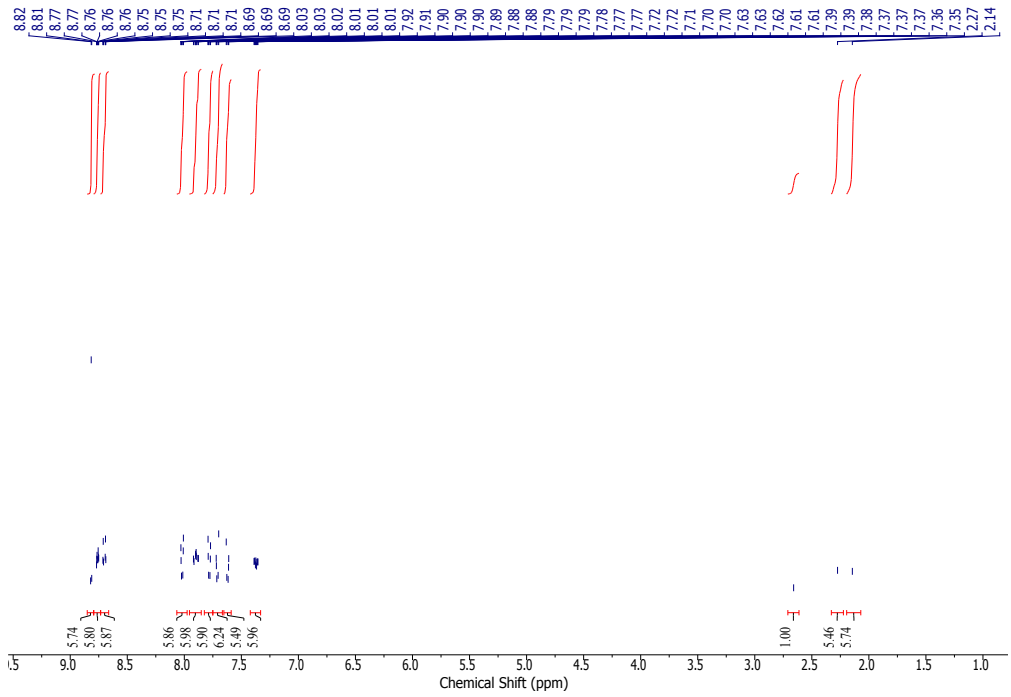

Figure S11. ^{1}H NMR (400 MHz) spectrum of **L1**

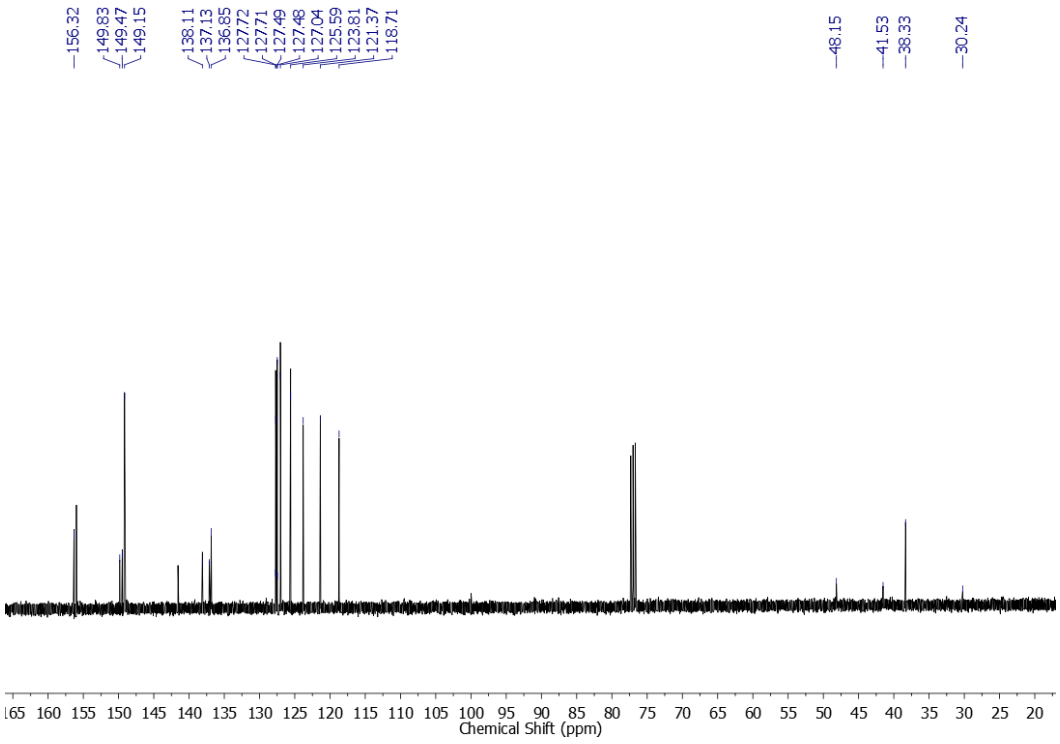

Figure S12. ^{13}C (400 MHz) NMR spectrum of **L1**

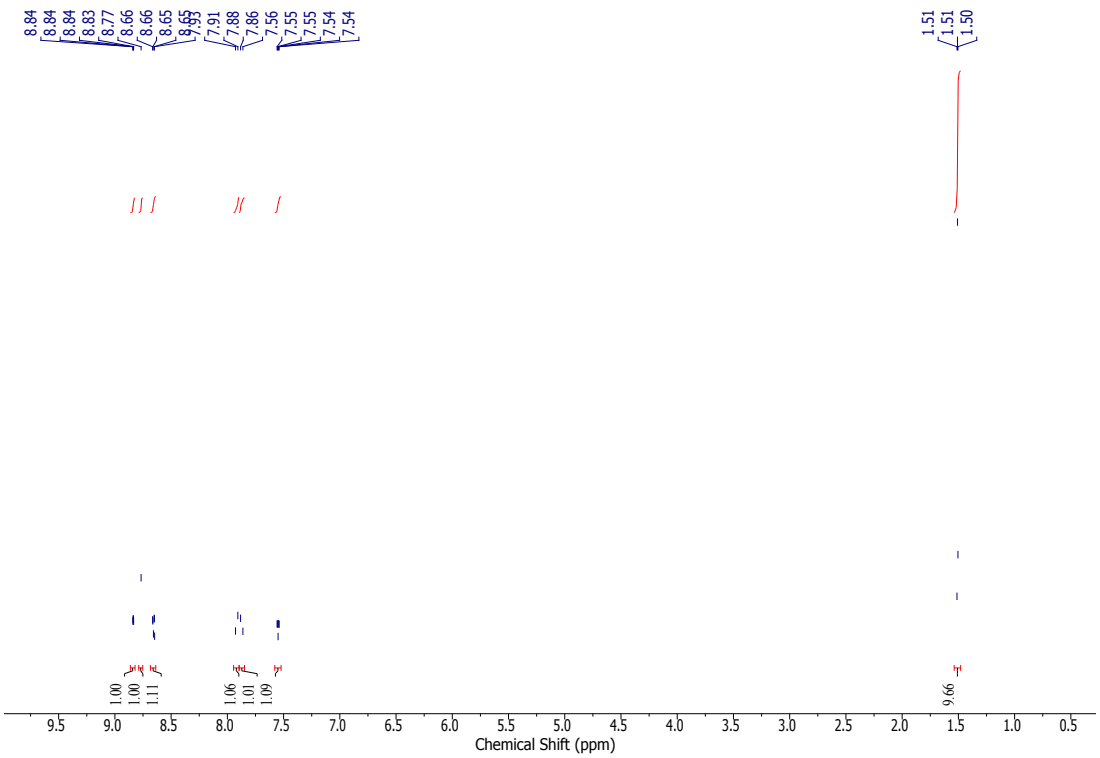

Figure S13. ^{1}H (400 MHz) NMR spectrum of **B2**

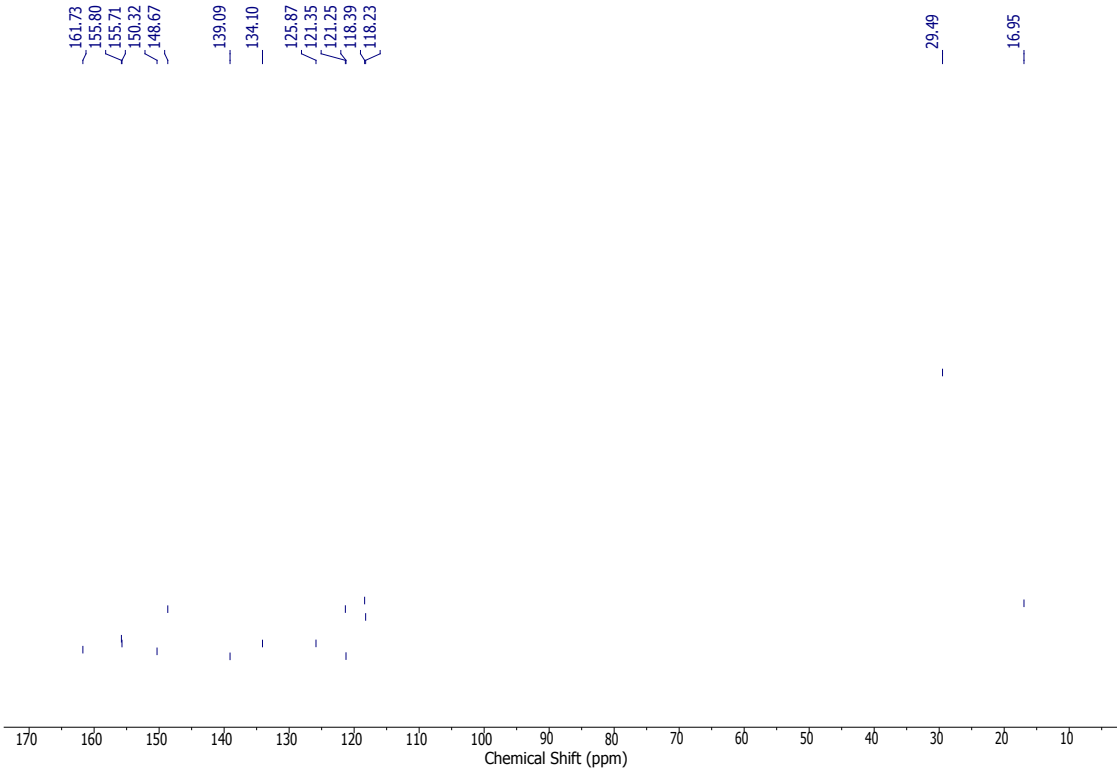

Figure S14. ^{13}C (400 MHz) NMR spectrum of **B2**

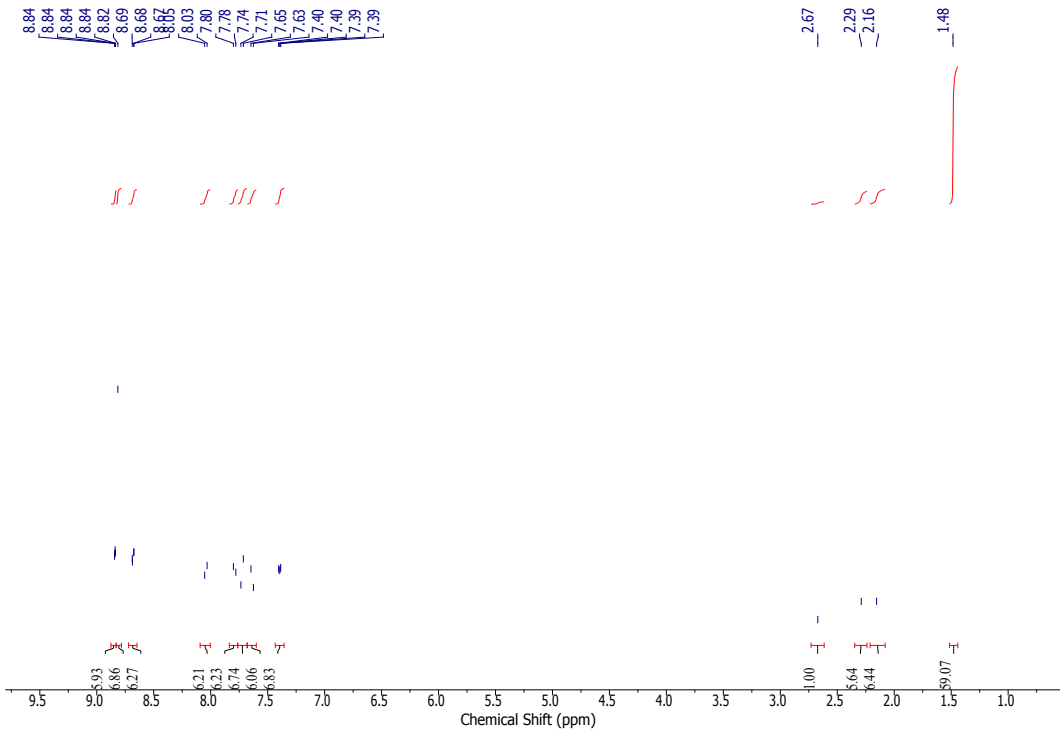

Figure S15. ^{1}H (400 MHz) NMR spectrum of **L2**

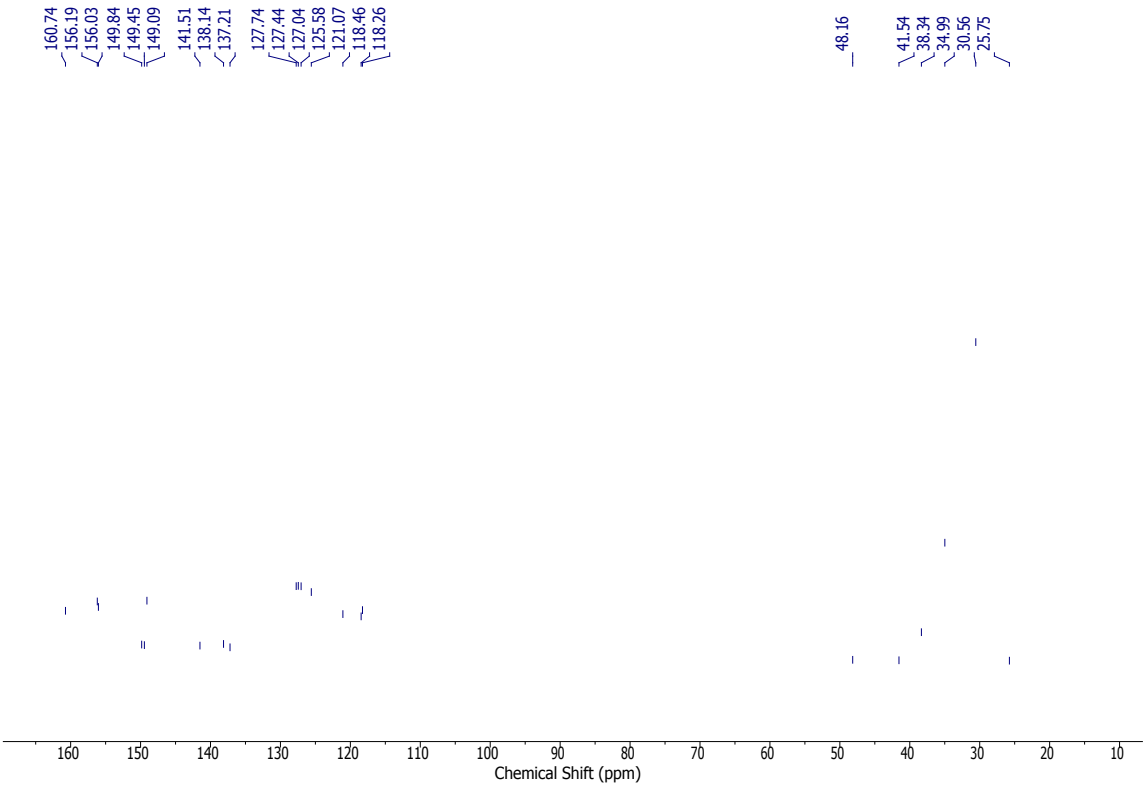

Figure S16. ^{13}C (400 MHz) NMR spectrum of **L2**

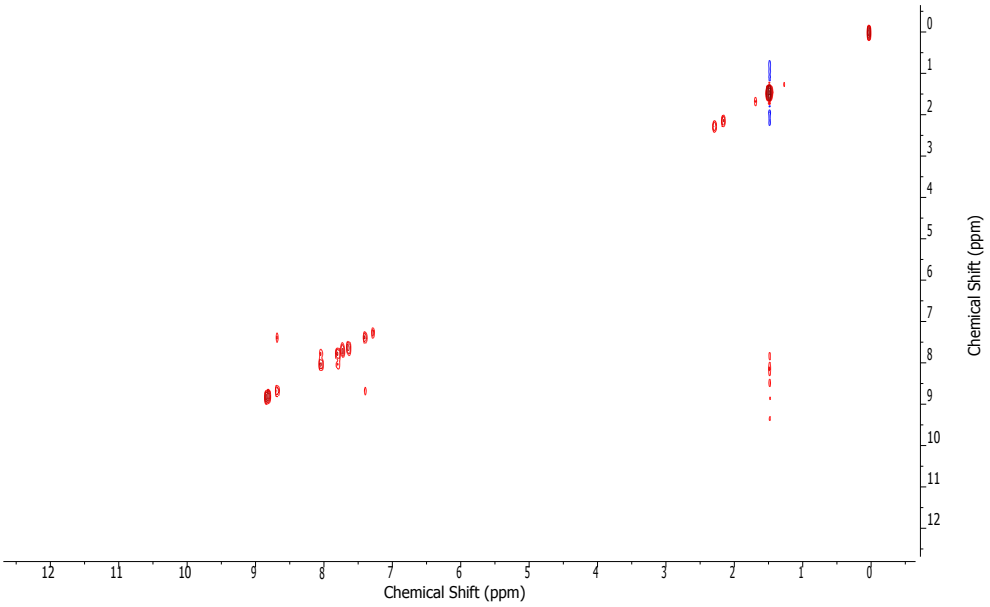

Figure S17. 2D-COSY (400 MHz) NMR spectrum of **L2**

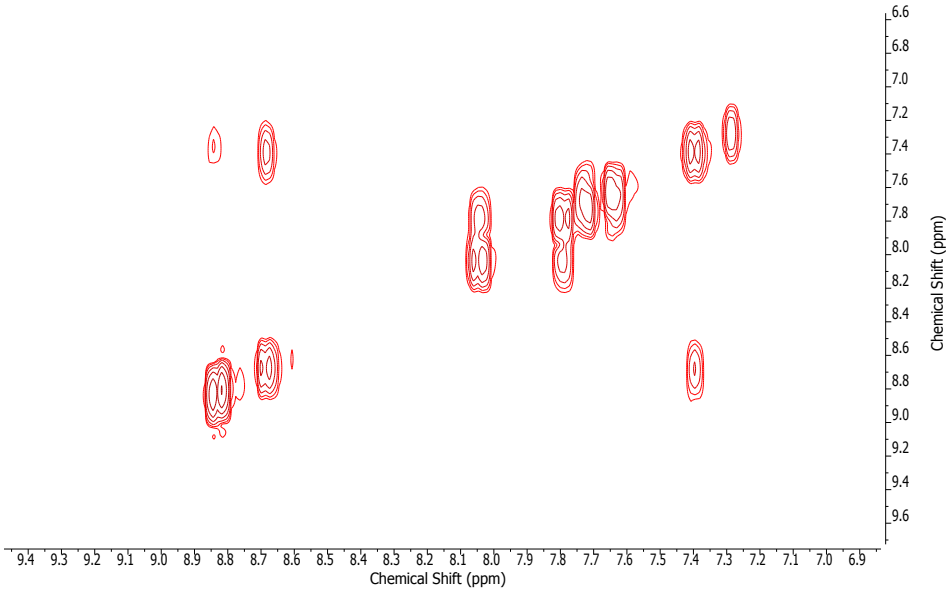

Figure S18. Enlarged 2D-COSY (400 MHz) NMR spectrum of **L2**

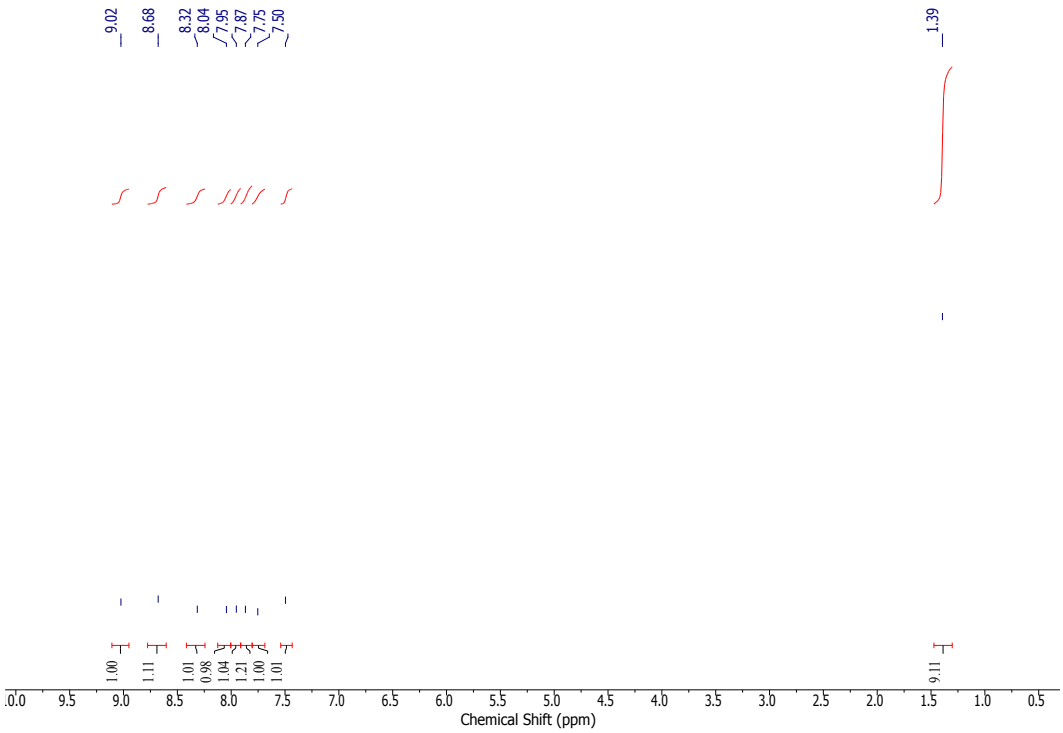

Figure S19. ^{1}H NMR (400 MHz) spectrum of [$\mathbf{Cd_{12}L2_8}$]

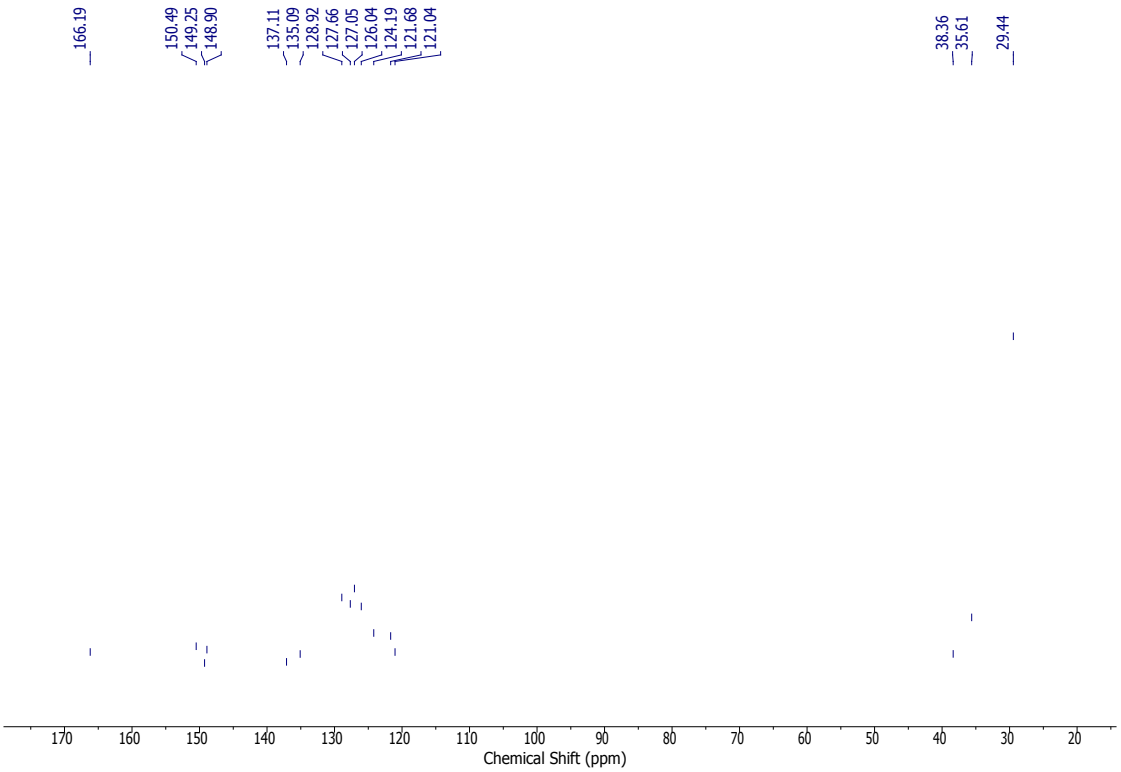

Figure S20. ^{13}C NMR (500 MHz) spectrum of [$\mathbf{Cd_{12}L2_8}$]

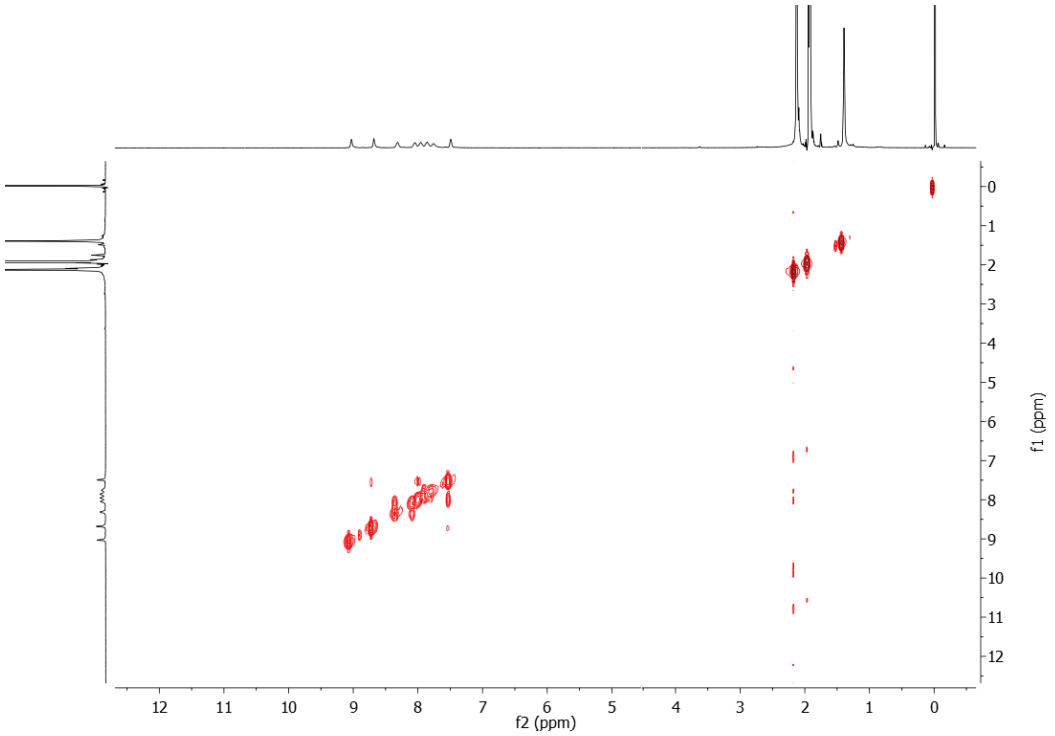

Figure S21. 2D-COSY (400 MHz) NMR spectrum of [$\mathbf{Cd_{12}L2_8}$]

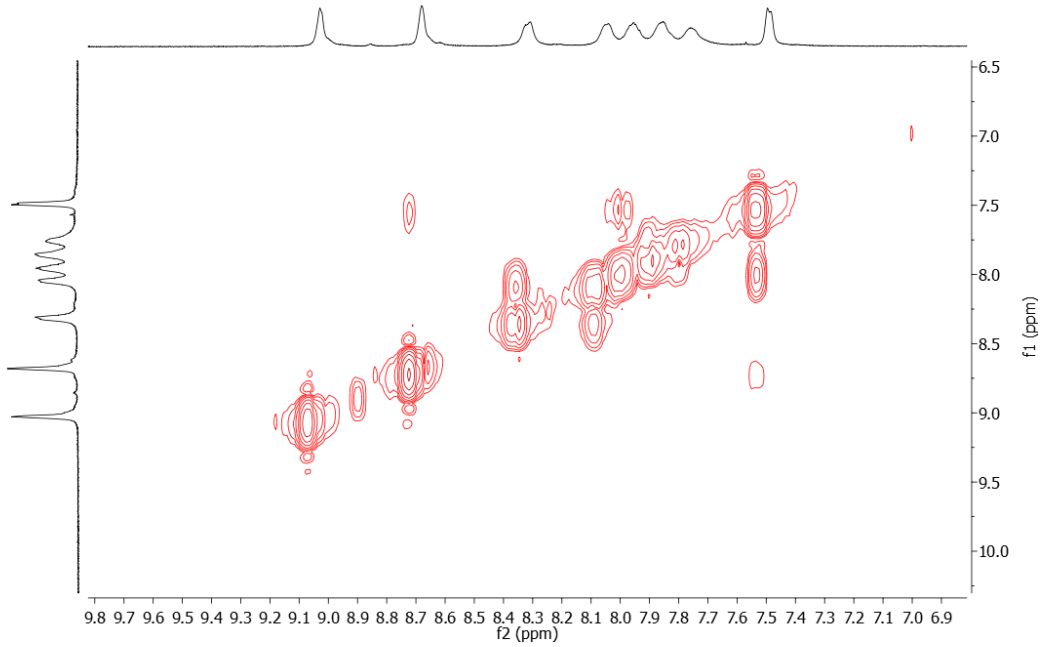

Figure S22. Enlarged 2D-COSY (400 MHz) NMR spectrum of [$\mathbf{Cd_{12}L2_8}$]

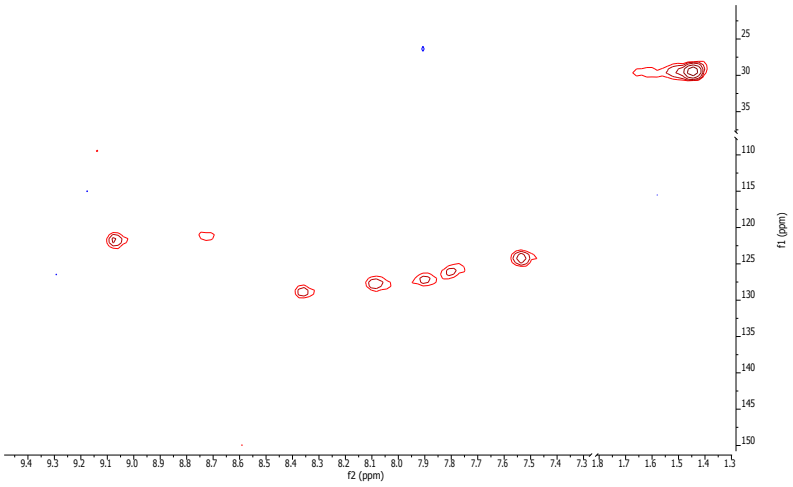

Figure S23. 2D-HSQC (500 MHz) NMR spectrum of [$\mathbf{Cd_{12}L2_8}$]

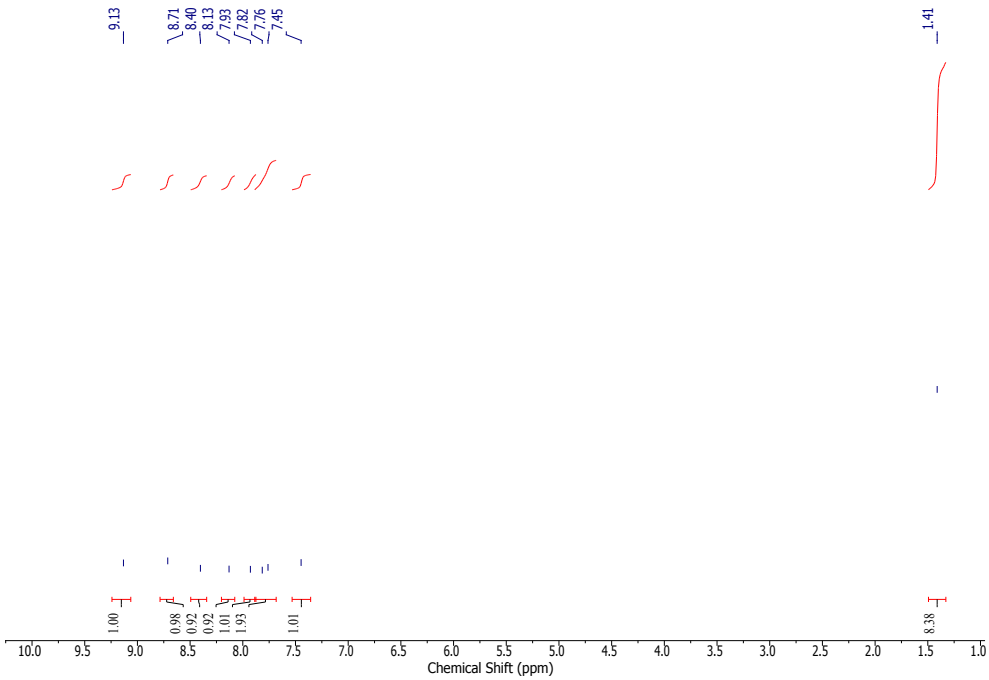

Figure S24. ^{1}H NMR (400 MHz) spectrum of [$\mathbf{Zn_{12}L2_8}$]

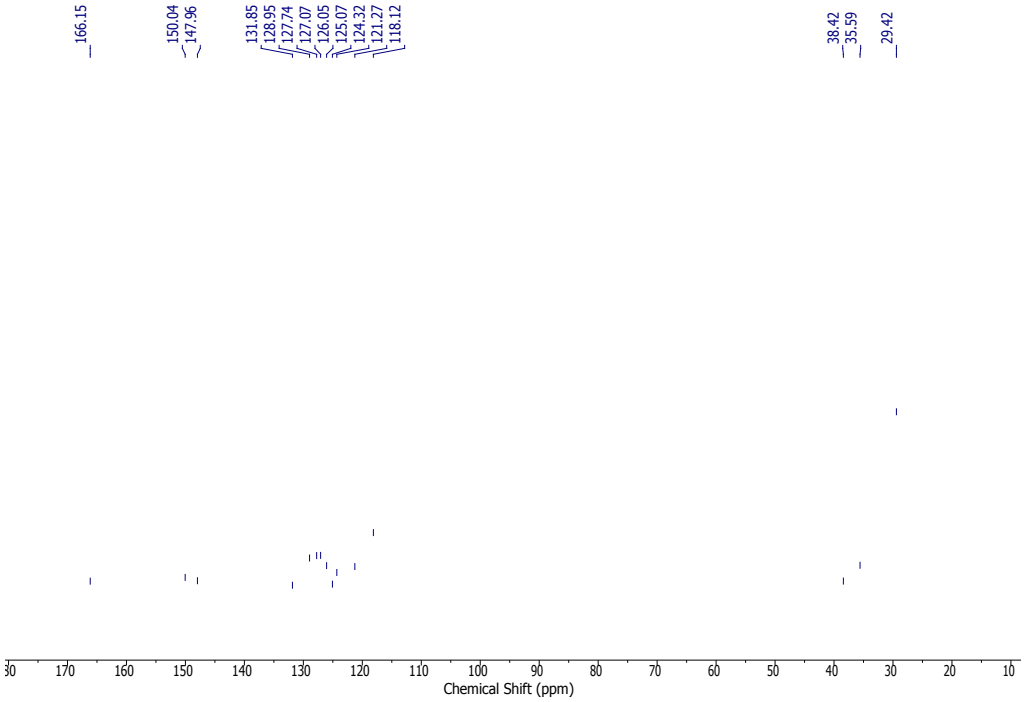

Figure S25. ^{13}C NMR (500 MHz) spectrum of [$\mathbf{Zn_{12}L2_8}$]

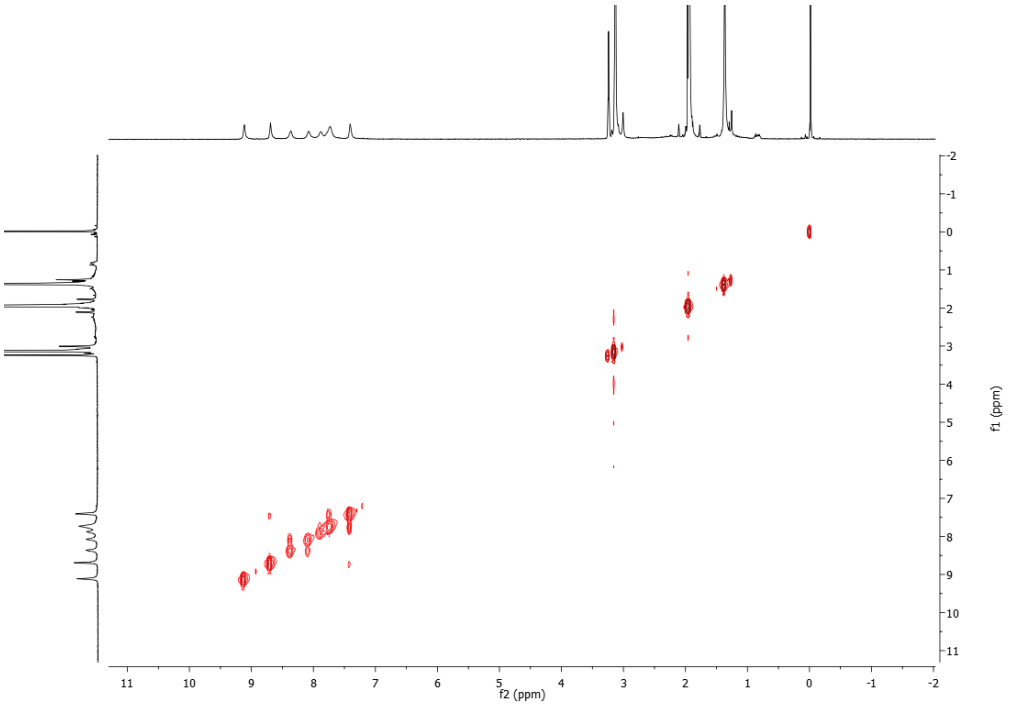

Figure S26. 2D-COSY (400 MHz) NMR spectrum of [$\mathbf{Zn_{12}L2_8}$]

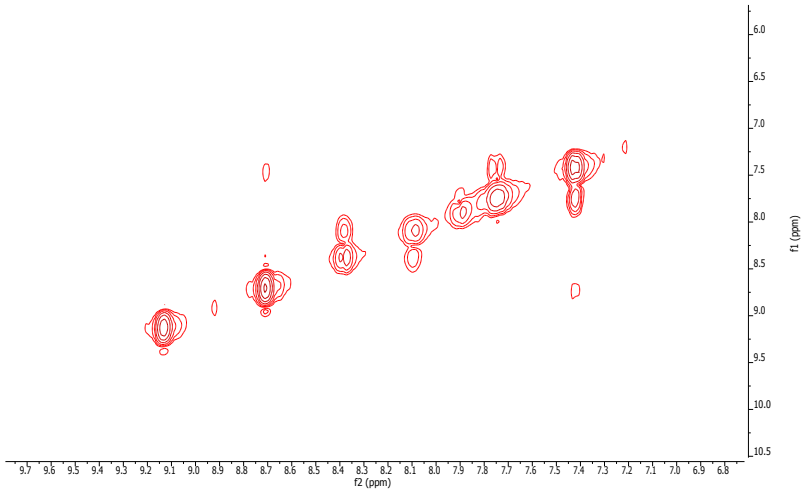

Figure S27. Enlarged 2D-COSY (400 MHz) NMR spectrum of [$\mathbf{Zn_{12}L2_8}$]

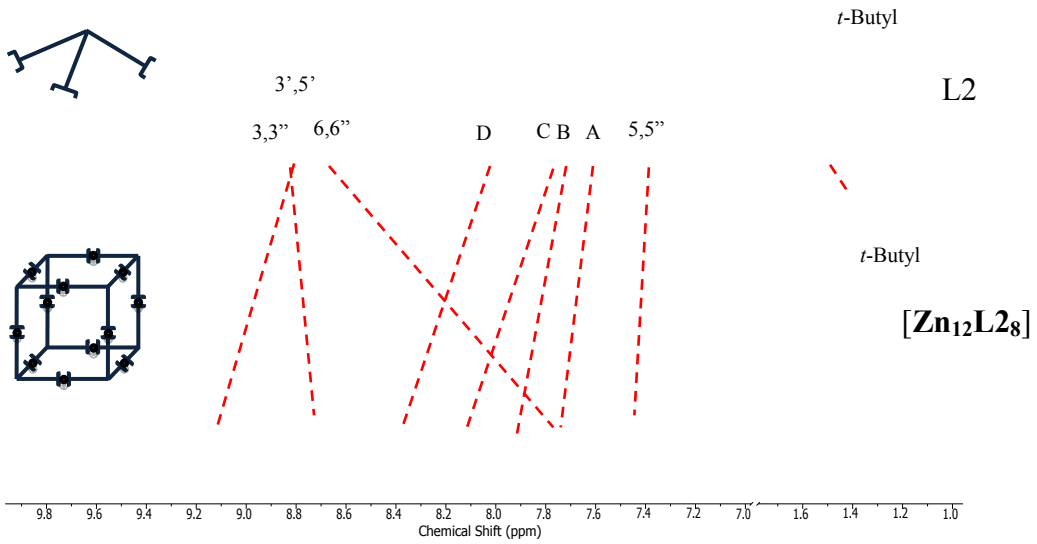

Figure S28. ^{1}H NMR spectra (400 MHz) of ligand **L2** in $CDCl_3$ and [$\mathbf{Zn_{12}L2_8}$] in CD_3CN.

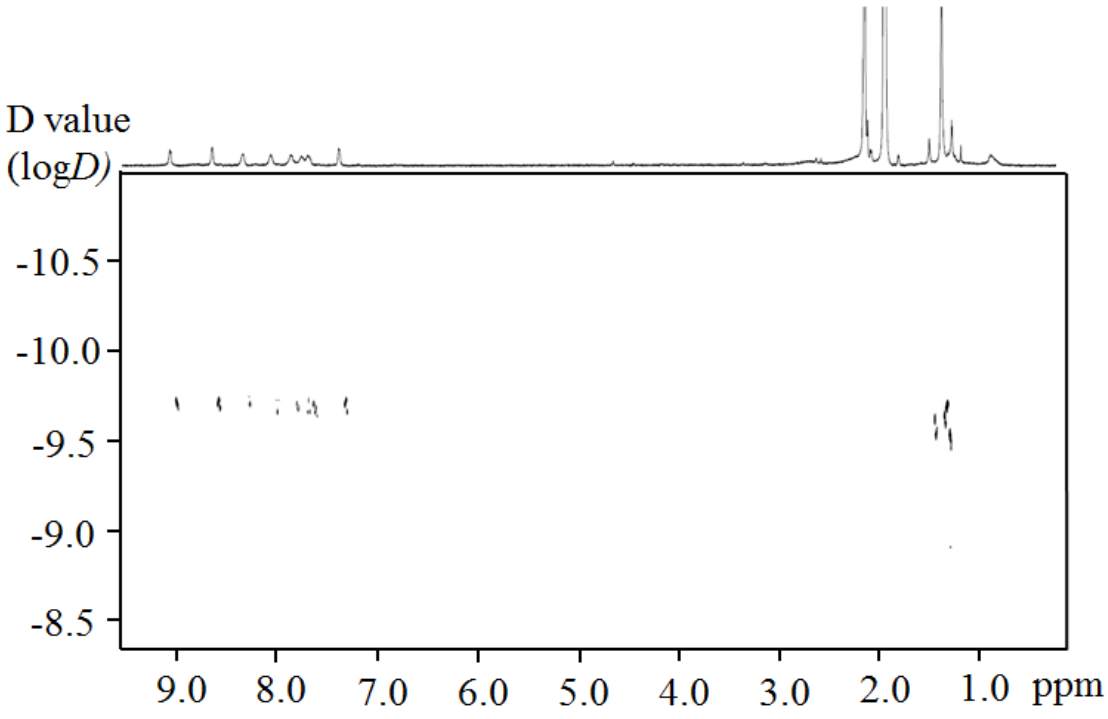

Figure S29. 2D-DOSY (500 MHz) NMR of [$\mathbf{Zn_{12}L2_8}$] in CD_3CN.

AFM results

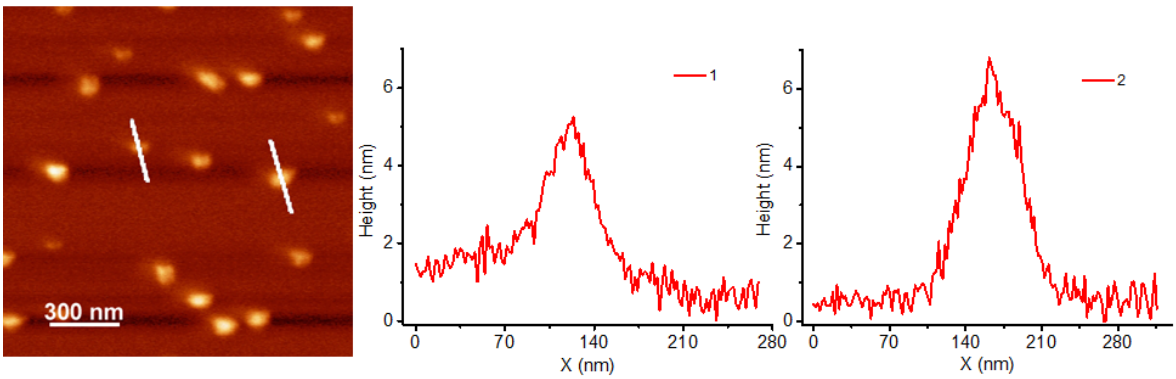

Figure S30. (left) AFM image of [$\mathbf{Cd_{12}L2_8}$] on mica surface and (right) Statistical histogram.

[$\mathbf{Cd_{12}L2_8}$] solution (10 μg/mL in MeCN) was dropped on freshly cleaved mica surface and dried in the air for AFM image. AFM imaging was carried out with an Agilent 5500 AFM system (Agilent, Chandler, AZ). Silicon cantilevers tip with spring constant of around 0.1 N/m were used for experiments. The image was obtained in air and was acquired by using Agilent magnetic AC (MAC) mode AFM with a magnetically coated cantilever. The obtained AFM image was processed by WSxM software.[7]

The images from atomic force microscopy (AFM) showed the morphology of the cube-like complex [$\mathbf{Cd_{12}L2_8}$] as dots on the mica surface (Figure S29). Some of the dots displayed cube-like shape. Due to the unavoidable tip broadening effect, the measured width of the dots in AFM image displayed large values.[8]

8. References

(1) Newman, H. *Synthesis* **1972**, *1972*, 692.

(2) Chin, D. N.; Gordon, D. M.; Whitesides, G. M. *J. Am. Chem. Soc.* **1994**, *116*, 12033.

(3) Wang, J.-L.; Li, X.; Lu, X.; Hsieh, I. F.; Cao, Y.; Moorefield, C. N.; Wesdemiotis, C.; Cheng, S. Z. D.; Newkome, G. R. *J. Am. Chem. Soc.* **2011**, *133*, 11450.

(4) Perera, S.; Li, X.; Soler, M.; Schultz, A.; Wesdemiotis, C.; Moorefield, C. N.; Newkome, G. R. *Angew. Chem. Int. Ed.* **2010**, *49*, 6539.

(5) Thalassinos, K.; Grabenauer, M.; Slade, S. E.; Hilton, G. R.; Bowers, M. T.; Scrivens, J. H. *Anal. Chem.* **2008**, *81*, 248.

(6) Fernandez-Lima, F. A.; Blase, R. C.; Russell, D. H. *Int. J. Mass spectrom.* **2010**, *298*, 111.

(7) Horcas, I.; Fernandez, R.; Gomez-Rodriguez, J. M.; Colchero, J.; Gomez-Herrero, J.; Baro, A. M. *Rev. Sci. Instrum.* **2007**, *78*, 013705.

(8) (a) Radmacher, M.; Fritz, M.; Hansma, H.; Hansma, P. *Science* **1994**, *265*, 1577(b) Chen, G.; Zhou, J.; Park, B.; Xu, B. *Appl. Phys. Lett.* **2009**, *95*, 043103.